Journal of Materials and Environmental Sciences
ISSN : 2028-2508

JMES, 2017 Volume 8, Issue 11, Page 3834-3843

http://www.jmaterenvironsci.com/

Corrosion inhibition study of 2-(2, 4-dichlorophenyl) -6-Nitro-1, 4-dihydroquinoxaline for carbon steel in hydrochloric acid solution

F. Benhiba[1*], N. Lotfi[1], K. Ourrak[2], Z. Benzekri [3], H. Zarrok[1], A. Guenbour[4], S. Boukhris[3], A. Souizi[3], M. El Hezzat[5], I. Warad[6], R. Touir[7,8], A. Zarrouk[9], H. Oudda[1]

[1] *Laboratory of Separation Processes, Faculty of Science, University IbnTofail, Kenitra, Morocco.*

[2] *Laboratory of Chemistry Physical, Faculty of Science, University Moulay Ismail, Meknès, Morocco.*

[3] *Laboratory of Organic Synthesis, Organometallic and Theoretical, Faculty of Science, University Ibn Tofail, Kenitra, Morocco*

[4] *Laboratory of Electrochemistry, Corrosion and Environment, Faculty of science, Rabat, Morocco.*

[5] *Laboratory of Chemistry Physical of Vitreous and Crystallized Materials, Faculty of Science, University IbnTofail, Kenitra, Morocco.*

[6] *Department of Chemistry, AN-Najah National University P.O. Box 7, Nablus, Palestine*

[7] *Laboratoire d'Ingénierie des Matériaux et d'Environnement : Modélisation et Application, Faculté des Sciences, Université Ibn Tofail, BP 133, Kénitra 14 000, Morocco.*

[8] *Centre Régional des Métiers de l'Education et de la Formation (CRMEF), Avenue Allal Al Fassi, Madinat Al Irfane BP 6210 Rabat, Morocco.*

[9] *LC2AME, Faculty of Science, First Mohammed University, PO Box 717, 60 000 Oujda, Morocco.*

Received 19 Feb 2017,
Revised 19 Jun2017,
Accepted 21 Jun 2017

Keywords
- ✓ Carbon steel;
- ✓ Corrosion inhibition;
- ✓ Electrochemical techniques;
- ✓ SEM.

F. Benhiba
benhibafouad@gmail.com

Abstract

The inhibitive effect and adsorption behavior of 2-(2,4-dichlorophenyl) -6-Nitro-1,4-dihydroquinoxaline (2ClN-Q) on carbon steel corrosion in 1M HCl solution at different temperatures were investigated using electrochemical measurements and Scanning electron microscopy (SEM) analysis. It is found that the inhibition efficiency increases with 2ClN-Q concentration and decreases with temperature. Polarization data showed that 2ClN-Q actes as mixed-type inhibitor, while EIS results revealed that the 2ClN-Q species adsorbes on the metal surface. This adsorption followed Langmuir adsorption isotherm. SEM studies revealed the formation of a protective film on the carbon steel surface such as indicated by EIS.

1. Introduction

Carbon steel is the most widely used as constructional material in many industries due to its excellent mechanical and low cost. It is used in large tonnages in marine applications, chemical processing, petroleum production and refining, construction and metal processing equipment. Acid solutions are widely used in industry, e.g., chemical cleaning, descaling, pickling, and oil-well acidizing, which leads to corrosive attack. Therefore, the use of inhibitors is one of the most common effective and economic methods to protect metals in acidic media [1-8]. The majority of the well-known inhibitors are organic compounds containing heteroatom, such as O, N, or S and multiple bonds, which allow an adsorption on the metallic surface [9-18].

The present investigation continues to focus on the application of new quinoxaline derivative, namely 2-(2,4-dichlorophenyl) -6-Nitro-1,4-dihydroquinoxaline (*2ClN-Q*) on carbon steel corrosion in acidic medium. Inspection of the structure of *2ClN-Q* in Fig. 1 reveals the presence of heteroatoms and aromatic rings which plays a significant role in corrosion inhibition of metals. This inhibition effect was evaluated by potentiodynamic polarization and electrochemical impedance spectroscopy techniques coupled with scanning electron spectroscopy.

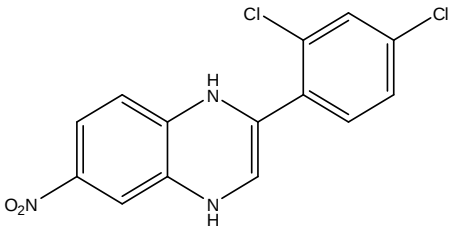

Figure1: Chemical structure of 2-(2,4-dichlorophenyl) -6-Nitro-1,4-dihydroquinoxaline (*2ClN-Q*).

2. Experimental

2.1. Materials

The steel used in this study is a carbon steel (CS) (Euronorm: C35E carbon steel and US specification: SAE 1035) with a chemical composition (in wt. %) of 0.370 % C, 0.230 % Si, 0.680 % Mn, 0.016 % S, 0.077 % Cr, 0.011 % Ti, 0.059 % Ni, 0.009 % Co, 0.160 % Cu and the remainder iron (Fe).

2.2. Solutions

The aggressive solutions of 1 M HCl were prepared by dilution of analytical grade 37 % HCl with distilled water. The concentration range of the used 2-(2,4-dichlorophenyl) -6-Nitro-1,4-dihydroquinoxaline (*2ClN-Q*) was 10^{-6} M to 10^{-3} M.

2.3. Electrochemical impedance spectroscopy

The electrochemical measurements were carried out using a Volta lab (Tacussel- Radiometer PGZ 100) potentiostate and controlled by Tacussel corrosion analysis software model (Voltamaster 4) at under static condition. The corrosion cell used had three electrodes. The reference electrode was a saturated calomel electrode (SCE). A platinum electrode was used as auxiliary electrode of surface area of 1 cm^2. The working electrode was carbon steel with the surface area of 1 cm^2. All potentials given in this study were referred to this reference electrode. The working electrode was immersed in test solution for 30 minutes to a establish steady state open circuit potential (Eocp). After measuring the Eocp, the electrochemical measurements were performed. All electrochemical tests have been performed in aerated solutions at 303 K. The EIS experiments were conducted in the frequency range with high limit of 100 kHz and different low limit 0.1 Hz at open circuit potential, with 10 points per decade, at the rest potential, after 30 min of acid immersion, by applying 10 mV ac voltage peak-to-peak. Nyquist plots were made from these experiments. The best semicircle can be fit through the data points in the Nyquist plot using a non-linear least square fit so as to give the intersections with the x-axis.

The inhibition efficiency of the inhibitor was calculated from the charge transfer resistance values using the following equation:

$$\eta_z\,\% = \frac{R_{ct}^{i} - R_{ct}^{\circ}}{R_{ct}^{i}} \times 100 \qquad (1)$$

Where, R_{ct}° and R_{ct}^{i} are the charge transfer resistance in the absence and presence of inhibitor, respectively.

2.4. Potentiodynamic polarization measurments

The electrochemical behaviour of carbon steel sample in uninhibited and inhibited solution was studied by recording anodic and cathodic potentiodynamic polarization curves. Measurements were performed in the 1 M HCl solution containing different concentrations of the tested inhibitor by changing the electrode potential automatically from - 800 to 0 mV/SCE at a scan rate of 1 mV s^{-1}. The linear Tafel segments of anodic and cathodic curves were extrapolated to corrosion potential to obtain corrosion current densities (i_{corr}) and the other parameters using the equation:

$$I = I_{corr}\left[exp\left(\frac{2.3\Delta E}{\beta_a}\right) - exp\left(\frac{2.3\Delta E}{\beta_c}\right)\right] \qquad (2)$$

The inhibition efficiency was evaluated from the determined i_{corr} values using the relationship:

$$\eta_{Tafel}\% = \frac{I^{\circ}_{corr} - I^{i}_{corr}}{I^{\circ}_{corr}} \times 100 \quad (3)$$

Where, I°_{corr} and I^{i}_{corr} are the corrosion current density in the absence and presence of inhibitor, respectively.

2.5. Scanning electron microscopy (SEM)

The morphology of surface state was performed using a JEOL JSM-5800 Scanning Electron Microscopy. The energy of the acceleration beam employed was 20 kV. The analysis by SEM was carried out on the surface of carbon steel samples before and after immersion in the acidic solutions without and with the optimal concentration of inhibitor.

3. Results and discussion

3.1. Electrochemical impedance spectroscopy measurements

The impedance responses of carbon steel in 1 M HCl in the absence and presence of *2ClN-Q* is depicted in Fig 2. It could be observed from the Nyquist plots that the impedance responses of carbon steel in the acid medium have not changed with *2ClN-Q* addition. These plots are characterized by one capacitive loop corresponding to one time constant suggesting that the carbon steel corrosion is controlled by a charge transfer process. The diameter of the semicircles in the Nyquist plot are observed to increase with *2ClN-Q* concentration suggesting the formation of an adsorption film on the carbon steel surface. This kind of deviations is often referred to as the frequency dispersion of interfacial impedance [19]. The anomaly is usually attributed to the inhomogeneity of the electrode surface arising from surface roughness or interfacial phenomena [19]. The electric equivalent circuit (EEC) model shown in Fig. 3 was used to model the physical processes taking place at the carbon steel /solution interface. The EEC consists of solution resistance (R_s), charge transfer resistance (R_{ct}) and constant phase element (CPE). The CPE is substituted for the capacitive element to give a more accurate fit as specified in the CPE impedance shown in the following equation:

$$Z_{CPE} = A^{-1}(\mathrm{i}\,\omega)^{-n} \quad (4)$$

$$C_{dl} = (AR_{ct}^{\,n-1})^{1/n} \quad (5)$$

where A is the coefficient of the proportionality in (Ω^{-1} S^n cm^{-2}), R_{ct} is the charge transfer resistance, ω is the angular frequency, of the imaginary number and n is an exponent associated with phase shift and which can be used as a measure of the irregularity of the surface. The double-layer capacitance C_{dl} values can be calculated with the use of constant phase element (CPE) settings [20,21]. The obtained impedance parameters and the inhibition efficiency are listed in Table 1. It is remarked that the inhibition efficiency increases with *2ClN-Q* concentration to reach a maximum of 88 % obtained at 10^{-3} M.

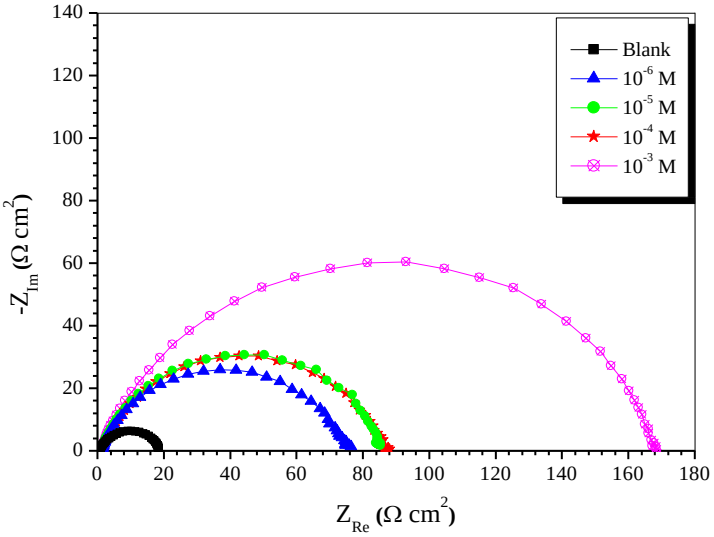

Figure2: Nyquist impedance diagram for carbon steel in 1 M HCl without and with different concentrations of *2ClN-Q* at 303 K.

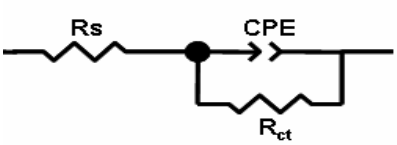

Figure3: Electric equivalent circuit of the metal / *2ClN-Q* / HCl.

Table 1. Electrochemical impedance parameters for carbon steel in 1 M HCl in the absence and presence of different concentrations of *2ClN-Q* at 303 K.

	Conc. (M)	R_s (Ω cm^2)	R_{ct} (Ω cm^2)	10^4 A (Ω^{-1} S^n cm^2)	n	C_{dl} (μF cm^{-2})	η_z (%)
Blank	1	0.54	20.27	4.45	0.850	193.8	--
2ClN-Q	10^{-6}	0.60	72.57	2.375	0.835	106.4	72.1
	10^{-5}	0.75	82.32	2,211	0.827	95.6	75.3
	10^{-4}	0.79	83.55	2.191	0.821	91.5	75.7
	10^{-3}	0.96	164.7	1.136	0.819	47.1	88.0

Data in the Table showed that the charge transfer resistance R_{ct} values increase and the double-layer capacitance values C_{dl} decrease with *2ClN-Q* concentration. The increase in R_{ct} was attributed to the formation of protective film on the metallic surface and the decrease in C_{dl} can be interpreted as a decrease in local dielectric constant and/or an increase in the thickness of the electrochemical double layer, which results from the adsorption of *2ClN-Q* molecules on the metallic surface [22]. In the other hand, the decrease in C_{dl} was in accordance with the Helmholtz model given by the following equation [23]:

$$C_{dl} = \frac{\varepsilon_o \varepsilon}{\delta} S \qquad (6)$$

where δ is the thickness of the protective layer, S the is the electrode area, ε_o is the vacuum permittivity of vide and ε is the dielectric constant of the medium.

3.2. Potentiodynamic polarization curves

Potentiodynamic polarization experiments were carried out potentiodynamically in order to gain insight into the kinetics of cathodic and anodic corrosion reactions. Fig. 4 shows the obtained potentiodynamic polarization curves for carbon steel in unstirred 1 M HCl in the absence and presence of different concentrations of *2ClN-Q*.

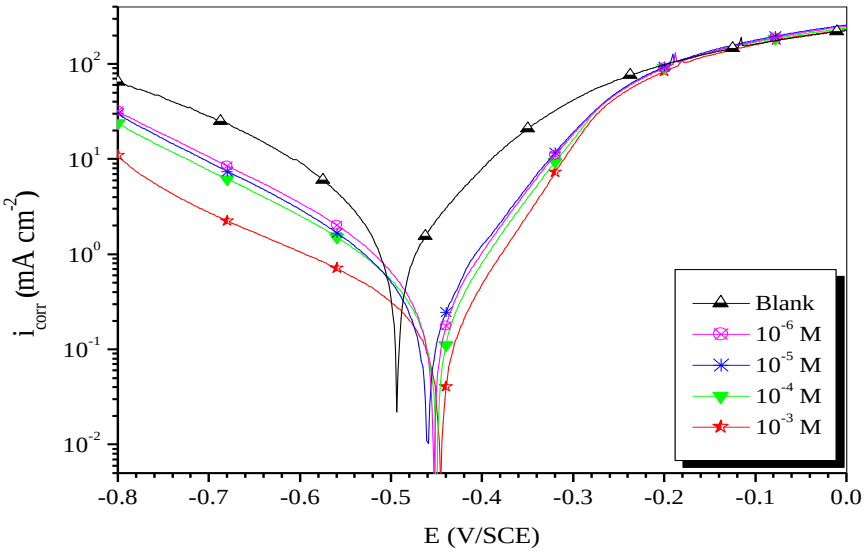

Figure4: Potentiodynamic polarization curves of carbon steel in 1 M HCl in the absence and presence of different concentrations of 2ClN-Q.

It can be observed from the figure that the carbon steel specimen exhibits active dissolution with no distinctive transition to passivation within the studied potential range in all environments. The electrochemical parameters such as corrosion current density (i_{corr}), corrosion potential (E_{corr}) and cathodic Tafel slope (β_c) are given in Table 2.

Table 2. Electrochemical parameters of carbon steel in 1 M HCl solution in the absence and presence of various concentrations of 2ClN-Q.

	Conc. (M)	$-E_{corr}$ (mV/SCE)	$-\beta_c$ (mV dec^{-1})	i_{corr} (μA cm^{-2})	η_{Tafel} (%)	Θ
Blank	00	469	140	588.0	—	—
Q1	10^{-6}	456	96	125.1	78.7	0.787
	10^{-5}	462	101	97.2	83.4	0.834
	10^{-4}	449	103	95.0	83.8	0.838
	10^{-3}	448	112	73.1	88.0	0.880

Some authors [24, 25] have pointed out that if the displacement of corrosion potential is more than 85 mVversus corrosion potential of blank solution, the inhibitor can be classified as a cathodic or anodic type. In our study, the maximum displacement in the presence of inhibitor is about 21 mV; therefore, the 2ClN-Q can be classified as a mixed-type inhibitor. This result also suggests that the inhibition is most probably caused by a geometric blocking effect of the adsorbed inhibitive species on the corroded metallic surface since the shift in corrosion potential is negligible in the presence of inhibitor [26].

3.3. Effect of temperature

Generally, the corrosion rates of mild steel in acidic solutions increase with rise in temperature. This is due to a decrease in the hydrogen evolution overpotential, resulting to the higher dissolution rates of metals. A higher rate of hydrogen gas generation increasingly agitates the metal-corrodent interface and depending on the nature of the metal/inhibitor interactions, could hinder inhibitor adsorption, perturb already adsorbed inhibitor or actually enhance inhibitor adsorption. In order to understud the temperature dependence of corrosion rates in uninhibited and inhibited solutions, potentiodynamic polarization measurement was carried out in the temperature range 303-333 K in the absence and presence of 10^{-3} M of 2ClN-Q.

Fig. 5a and 5b present the obtained potentiodynamic polarization curves for carbon steel electrode in 1 M HCl, without and with 10^{-3} M of 2ClN-Q at different temperature. The respective kinetic parameters are given in Table 3. It was found that the corrosion rate of carbon steel in free and inhibited solutions increases with temperature. In addition, it is shown that the inhibition efficiency decreases with temperature. These results confirm that this inhibitor acts as an effective inhibitor in the studied temperature range.

The apparent activation energy, E_a of the corrosion reaction was determined using the Arrhenius equation:

$$I_{corr} = A\exp\left(\frac{-E_a}{RT}\right) \quad (7)$$

where i_{corr} is the corrosion current density, E_a is the apparent activation energy of the corrosion reaction and A is the Arrhenius pre-exponential factor. The apparent activation energy of the corrosion reaction in the absence and presence 10^{-3} M of 2ClN-Q could be determined by plotting Ln (i_{corr}) with 1/T which gives a straight line (Fig. 6) with a slope permitting the determination of E_a. Fig. 6 shows the Arrhenius plots in the absence and presence of 10^{-3} M of 2ClN-Q. The corresponding values of E_a are given in Table 4 and indicate that the obtained value of E_a in solution containing 2ClN-Q is higher than those in the inhibitor-free acid solution. This finding coupled with the observed decrease in inhibition efficiency with temperature suggest that the 2ClN-Q could be physisorbed on the carbon steel surface [27,28].

An alternative formulation of Arrhenius equation (Eyring transition state equation) is [29]:

$$I_{corr} = \frac{RT}{Nh}\exp\left(\frac{\Delta S_a}{R}\right)\exp\left(\frac{\Delta H_a}{RT}\right) \quad (8)$$

where h is the Planck's constant, N_A is the Avogadro's number, R is the universal gas constant, ΔH_a is the enthalpy of the activation and ΔS_a is the entropy of activation.

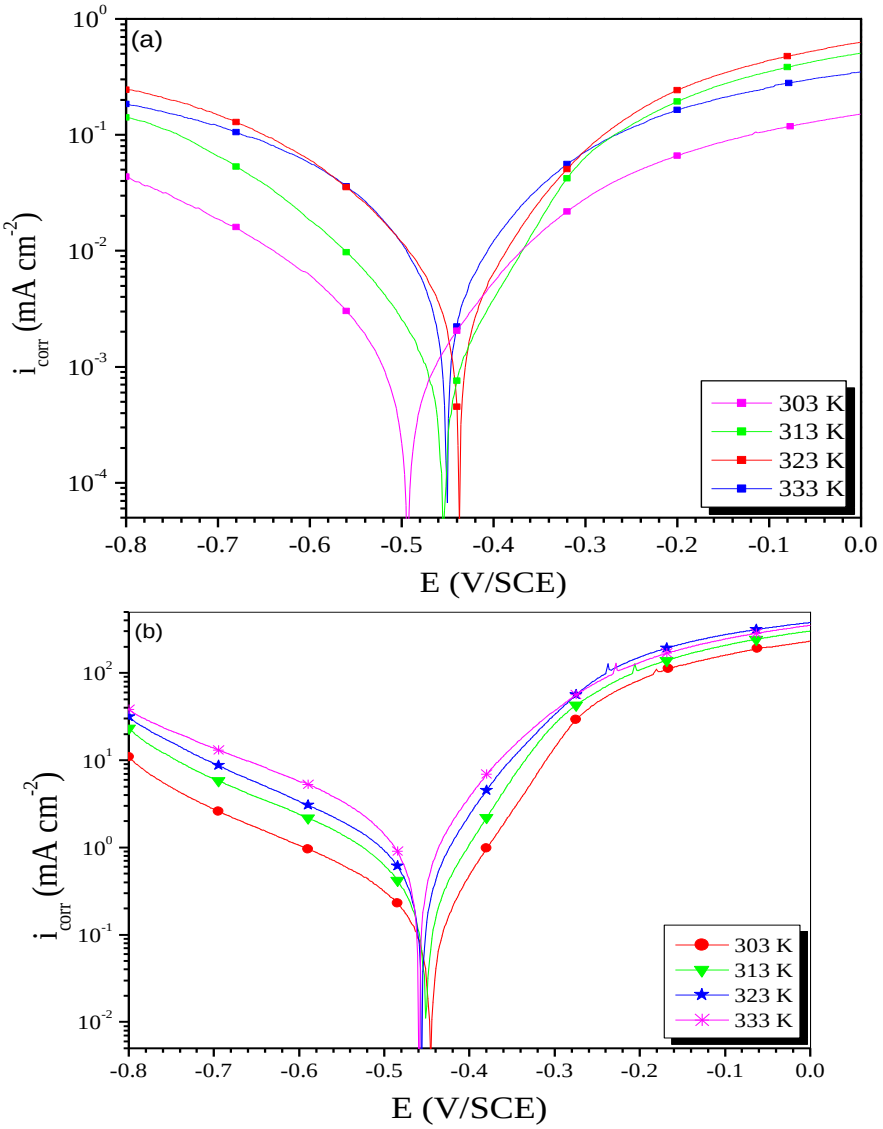

Figure 5: Effect temperature on the potentiodynamic polarization curves of carbon steel in 1 M HCl at different temperature range (a) without and (b) with 10^{-3} M of 2ClN-Q.

Table 3. Electrochemical parameters and corresponding inhibition efficiencies for carbon steel in 1M HCl without and with 10^{-3} M of 2ClN-Q at different temperatures.

	T (K)	$-E_{corr}$ (mV/SCE)	$-\beta_c$ (mV dec^{-1})	i_{corr} (µA cm^{-2})	η_{Tafel} (%)
Blank	303	469	168	588	—
	313	467	165	896	—
	323	470	137	2610	—
	333	477	125	5100	—
10^{-3} M of 2ClN-Q	303	449	118	35	94.0
	313	477	102	118	87.0
	323	476	87	350	86.5
	333	474	60	700	86.2

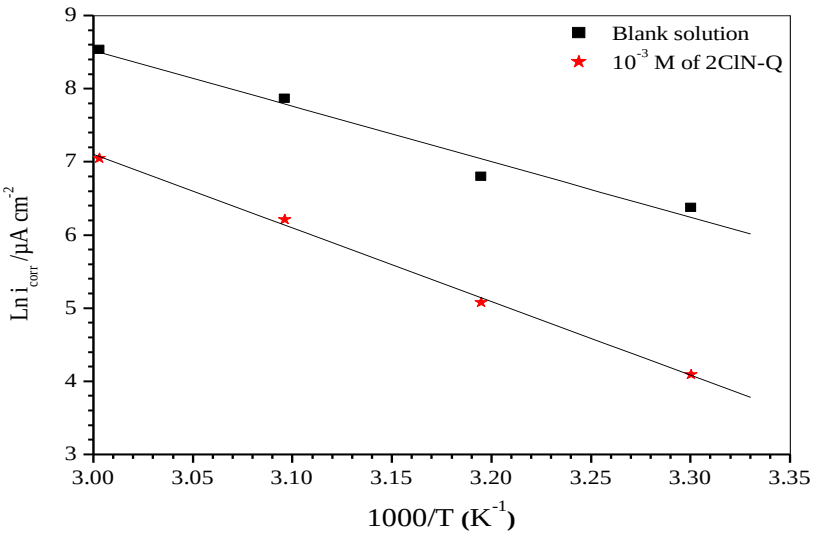

Figure6: Arrhenius plots of carbon steel in 1 M HCl without and with 10^{-3} M of 2ClN-Q.

Table 4. Activation parameters, E_a, ΔH_a and ΔS_a, of the carbon steel dissolution in 1 M HCl without and with 10^{-3} M of 2ClN-Q.

	E_a (kJ mol^{-1})	ΔH_a (kJ mol^{-1})	ΔS_a (J mol^{-1} K^{-1})
Blank	63.1	60.4	- 6.5
10^{-3} M of 2ClN-Q	83.8	81.1	-56.7

The values of enthalpy and entropy of activation for carbon steel corrosion in 1M HCl in the absence and presence of 2ClN-Q can be evaluated from the slope and intercept of the curve of Ln (i_{corr}/T) versus 1/T, respectively as shown in Fig. 7.

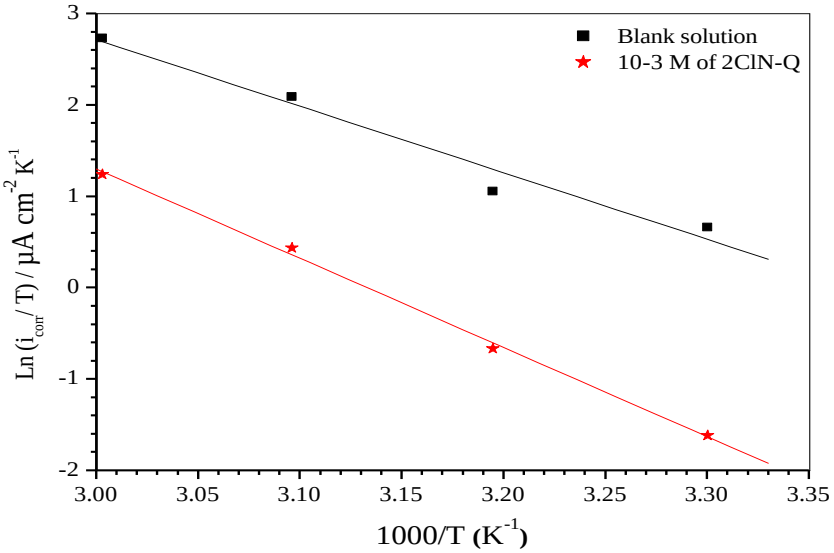

Figure7: Transition Arrhenius plots of carbon steel in 1 M HCl without and with 10^{-3} M of 2ClN-Q.

The positive sign of ΔH_a reflects the endothermic nature of the carbon steel dissolution process suggesting that the dissolution of carbon steel is slow [30] in the presence of inhibitor. The entropy of activation in the absence and presence of 2ClN-Q are large and negative. This implies that the activated complex in the rate-determining step represents association rather than dissociation, indicating that a decrease in disorder takes place, going from reactant to the activated complex [31-33].

3.4. Adsorption isotherm

In general, an adsorption isotherm is an invaluable curve describing the phenomenon governing the retention or release of substances from the aqueous porous media to a solid phase at constant temperature. Adsorption equilibrium (the ratio between the adsorbed amount with that remaining in solution) is established when an adsorbate containing phase is in contact with the adsorbent for sufficient time. From this point of view, the current model has excellence in that it has only fitting parameter that quantifies the concentration dependence of adsorption. In our present investigation, attempts were made to fit to various isotherms which are expressed as [34,35]:

Temkin isotherm : $\exp(f\theta) = K_{ads}C$ (9)

Langmuir isotherm : $\theta = K_{ads}C$ (10)

Frumkin isotherm : $\left(\frac{\theta}{1-\theta}\right)\exp(-2f\theta) = K_{ads}C$ (11)

Freundlich isotherm : $Log\,\theta = LogK_{ads} + nLogC$ (12)

where K_{ads} is the binding constant of adsorption, C is the inhibitor concentration, f is the factor of energetic inhomogeneity, θ is the degree of surface coverage wich calculated using the following formula:

$$\theta = \frac{I^{\circ}_{corr} - I^{i}_{corr}}{I^{\circ}_{corr}} \quad (13)$$

For obtaining the best description of adsorption behavior of the 2ClN-Q, all the above adsorption isotherms equations were tested. The plot of C/θ versus C yielded acceptable correlation coefficient value is 0.99997 with slope near to 1.1, which suggests that the adsorption of the 2ClN-Q molecules on the carbon steel surface obeys to the Langmuir adsorption isotherm as depicted in Fig. 8.

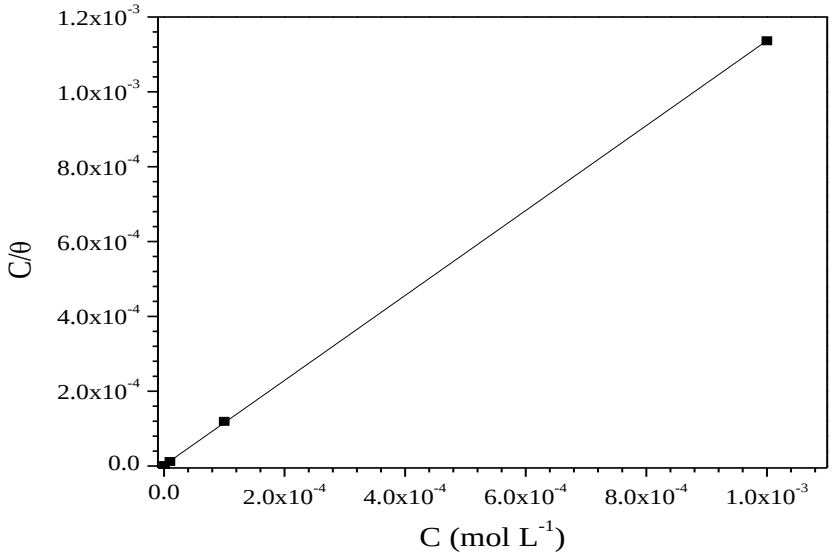

Figure8: Langmuir adsorption isotherm plot for 2ClN-Q in 1 M HCl solution at 303 K.

The binding constant of adsorption K_{ads} is related to the standard free energy of adsorption ($-\Delta G^{\circ}_{ads}$) by equation (14) [36]:

$$K_{ads} = \frac{1}{55.5}\exp\left(\frac{-\Delta G^{\circ}_{ads}}{RT}\right) \quad (14)$$

where the value 55.5 is the concentration of water in solution expressed in mol L^{-1}, R is the molar gas constant (8.3143 J K^{-1} mol^{-1}), and T is the absolute temperature.

It is generally accepted that the values of $-\Delta G^{\circ}_{ads}$ up to -20 kJ mol^{-1} are accordant with electrostatic interaction between the charged molecules and the charged metal surface (physisorption) whereas those ranging -40 kJ

mol^{-1} or more negative involve charge sharing or transfer from the inhibitor molecules to the metal surface to form a coordinate type of bond (chemisorption) [37-41]. The obtained $-\Delta G^{\circ}_{ads}$ value is -40.1 kJ mol^{-1}, this value can be suggested that the interaction of the 2ClN-Q involves both physisorption and chemisorption [42].

3.5 Scanning electron microscopy analysis

Fig. 9 shows the micrographs obtained by SEM of the carbon steel surface before and after immersion for 6 h in the blank solution without and with 10^{-3} M of 2ClN-Q. Comparing Figs. 9a and b, the latter shows strong damage on its surface without the presence of the inhibitor. Nevertheless, Fig. 9c shows how the 2ClN-Q has surface protective properties, revealing that the protective film is responsible for diminishing the damage caused.

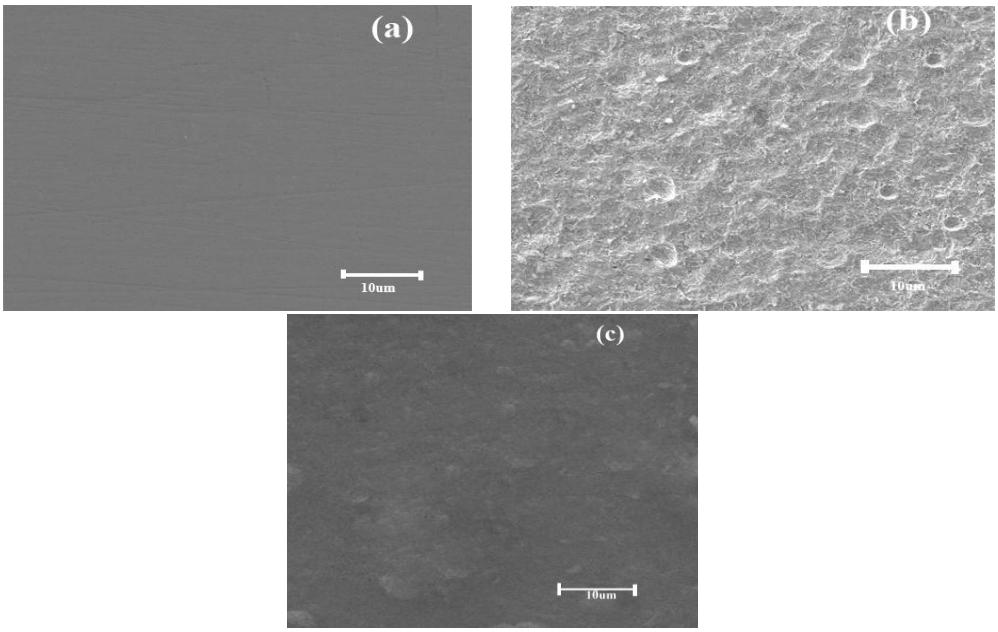

Figure9: Micrographs SEM at 303 K surface of carbon steel: (a) before immersion, (b) after 6 h of immersion in blank solution and (c)) after 6 h of immersion in blank solution in the presence of 10^{-3}M of 2ClN-Q.

Conclusion

This study has revealed that 2ClN-Q acts as a good inhibitor of carbon steel corrosion in 1 M HCl solutions. Potentiodynamic polarization studies showed that this compound acts as mixed-type inhibitor.It is found that the inhibition efficiency increases with increasing inhibitor concentration. In addition, EIS plots indicated that the charge transfer resistances increase with inhibitor concentration to reach a maximum at 10^{-3} M. It is found also that the 2ClN-Q inhibits corrosion by getting adsorbed on the metal surface following Langmuir adsorption isotherm. SEM micrographs indicated that the studied inhibitor acts by the formation of a protective film at the metallic surface.

References

1. Aouine Y., Sfaira M., Ebn Touhami M., Alami A., Hammouti B., Elbakri M., El Hallaoui A., Touir R., *Inter. J. Electrochem.* 7 (2012) 5400-5419.
2. Afrine L., Zarrouk A., Zarrok H., Salghi R., Touir R., Hammouti B., Oudda H., Assouag M., Hannache H., El Harti M., Bouachrine M., *J. Chem. Pharm. Res.* 5 (2013) 1474-1481.
3. El Hezzat M., Assouag M., Zarrok H., Benzekri Z., El Assyry A., Boukhris S., Souizi A., Galai M., Touir R., Ebn Touhami M., Oudda H., Zarrouk A., *Der Pharma Chemica.* 7 (2015) 77-88.
4. Benhiba F., Zarrok H., Elmidaoui A., El Hezzat M., Touir R., Guenbour A., Zarrouk A., Boukhris S., Oudda H., *J. Mater. Environ. Sci.* 6 (2015) 2301-2314.
5. Elbakri M., Touir R., Ebn Touhami M., Zarrouk A., Aouine Y., Sfaira M., Bouachrine M., Alami A., El Hallaoui A., *Res. Chem. Interm.* 39 (2013) 2417-2433.

6. Ghazoui A., Saddik R., Benchat N., Hammouti B., Guenbour M., Zarrouk A., Ramdani M., *Der Pharm. Chem.* 4(1)(2012) 352.
7. Zarrok H., Saddik R., Oudda H., Hammouti B., El Midaoui A., Zarrouk A., Benchat N., Ebn Touhami M., *Der Pharm. Chem*. 3(5)(2011)272.
8. Zarrouk A., Hammouti B., Touzani R., Al-Deyab S.S., Zertoubi M., Dafali A., Elkadiri S., *Int. J. Electrochem. Sci*.6 (10)(2011) 4939.
9. Zarrouk A., Hammouti B., Dafali A., Zarrok H., *Der Pharm. Chem.* 3(4) (2011)266.
10. Ghazoui A., Zarrouk A., Bencaht N., Salghi R., Assouag M., El Hezzat M., Guenbour A., Hammouti B., *J. Chem. Pharm. Res*. 6(2) (2014)704.
11. Zarrok H., Zarrouk A., Salghi R., Oudda H., Hammouti B., Assouag M., Taleb M., Ebn Touhami M., Bouachrine M., Boukhris S., *J. Chem. Pharm. Res*. 4(12) (2012)5056.
12. Zarrok H., Zarrouk A., Salghi R., Assouag M., Hammouti B., Oudda H., Boukhris S., Al Deyab S.S., Warad I., *Der Pharm. Lett.* 5(2) (2013)43.
13. Belayachi M., Serrar H., Zarrok H., El Assyry A., Zarrouk A., Oudda H., Boukhris S., Hammouti B., Ebenso E.E., Geunbour A., *Int. J. Electrochem. Sci*. 10(4) (2015)3010.
14. Zarrouk A., Zarrok H., Salghi R., Touir R., Hammouti B., Benchat N., Afrine L.L., Hannache, M. El Hezzat H., Bouachrine M., *J. Chem. Pharm. Res*. 5(12) (2013)1482.
15. Zarrok H., Zarrouk A., Salghi R., Ebn Touhami M., Oudda H., Hammouti B., Touir R., Bentiss F., Al-Deyab S.S., *Int. J. Electrochem. Sci*. 8(4) (2013)6014.
16. Touir R., Belakhmima R. A., Ebn Touhami M., Lakhrissi L., El Fayed M., Lakhrissi B., Essassi E. M., *J. Mater. Environ. Sci*., 4 (2013)921-930.
17. EL Aoufir Y., Lgaz H., Bourazmi H., Kerroum Y., Ramli Y., Guenbour A., Salghi R., El-Hajjaji F., Hammouti B., Oudda H., *J. Mater. Environ. Sci.* 7 (12) (2016) 4330-4347
18. Hammouti B., Zarrouk A., Al-Deyab S.S., Warad I., *Orient. J. Chem.* 27(2011) 23.
19. Martinez S., Metikoš-Huković M., *J. Appl. Electrochem.* 33(12) (2003) 1137.
20. Popova A., Sokolova E., Raicheva S., Christov M., *Corros. Sci*. 45 (2003)33.
21. Macdonald J.R., *Wiley, New York*. 1987.
22. Fu J., Li S., Wang Y., Cao L., Lu L., *J. Mater. Sci.* 45 (22) (2010) 6255.
23. Khaled K.F., Al-Qahtani M.M., *Mater. Chem. Phys.* 113(1) (2009)150.
24. Ferreira E.S., Giancomelli C.F., Giacomelliv, Spinelli A., *Mater. Chem. Phys*. 83 (2004)129.
25. Li W., He Q., Zhang S., Pei C., Hou B., *J. Appl. Electrochem*. 38(2008)289.
26. Cao C., *Corros. Sci*. 38(1996)2073.
27. Martinez S., Stern I., *Appl. Surf. Sci.* 199(2002) 83.
28. Szauer T., Brand A., *Electrochim. Acta*. 26(1981)1219.
29. Behpour M., Ghoreishi S.M., Mohammadi N., Soltani N., Salavati-Niasari M., *Corros. Sci*. 52(2010)4046.
30. Guan N.M., Xueming L., Fei L., *Mater. Chem. Phys*. 86(2004)59.
31. Ostovari A., Hoseinieh S.M., Peikari M., Shadizadeh S.R., Hashemi S.J., *Corros. Sci*. 51(2009)1935.
32. Martinez S., Stern I., *Appl. Surf. Sci*. 199(2002)83.
33. Marsh J., *Wiley Eastern, New Delh.* 1988.
34. Yadav D. K., Maiti B., Quraishi M. A., *Corros. Sci*. 52(2010) 3586.
35. Obi-Egbedi N.O., Essien K. E., Obot I.B., *J. Comput. Method Mol. Des*. 1(1) (2011)26.
36. Negm N.A., Kandile N.G., Aiad I. A., Mohammad M.A., *Colloids Surf. A*. 391(2011)224.
37. Negm N.A., Elkholy Y.M., Zahran M.K., Tawfik S.M., *Corros. Sci*. 52(2010)3523.
38. Obi-Egbedi N.O., Obot I.B., *Corros. Sci*. 53(2011)263.
39. Özcan M., Karadag FDehri., I., *Acta Physico-Chim. Sin*. 24(2008)1387.
40. Wang X., Yang H., Wang F., *Corros. Sci*. 53(2011)113.
41. Özcan M., Solmaz R., Kardasv, Dehri I., *Colloids Surf*. 325(2008)57.
42 Yang Z., Zhan F., Pan Y., LYu Z., Han C., Hu Y., Ding P., Gao T., Zhou X., Jiang Y., *Corros. Sci*. 99(2015)281.